Perfect Chirality with imperfect polarisation

Ben Lang,[1, *] Dara P. S. McCutcheon,[1] Edmund Harbord,[1] Andrew B. Young,[1] and Ruth Oulton[1]

[1] *Quantum Engineering Technology Labs, H. H. Wills Physics Laboratory and Department of Electrical & Electronic Engineering, University of Bristol, BS8 1FD, UK*

Unidirectional (chiral) emission of light from a circular dipole emitter into a waveguide is only possible at points of perfect circular polarisation (C points), with elliptical polarisations yielding a lower directional contrast. However, there is no need to restrict engineered systems to circular dipoles, and with an appropriate choice of dipole unidirectional emission is possible for any elliptical polarization. Using elliptical dipoles, rather than circular, typically increases the size of the area suitable for chiral interactions (in an exemplary mode by a factor ~ 30), while simultaneously increasing coupling efficiencies. We propose illustrative schemes to engineer the necessary elliptical transitions in both atomic systems and quantum dots.

Introduction - Nanostructures are often employed to finely control light. A common application is confining light into narrow channels to maximise the interaction probability between photons and a matter system, such an atom or quantum dot (QD) located at the focus point, a situation sometimes called the "1D atom" [1–3]. The light propagating through these narrow channels has components of transversely rotating ("rolling") electric fields [4], a consequence of Gauss' law [5]. This rolling polarisation can give rise to *chirality*, a near-field effect where atomic transitions described by circular dipoles radiate in a preferred direction [6–9].

These chiral behaviours have been recognised as a new tool in the development of light-matter interfaces [10]. One application is constructing on-chip quantum memories with charged QDs, the qubit-states of which possess oppositely handed circular dipoles. Without chirality distinguishing these dipoles in-plane is cumbersome: requiring the collection and interference of beams propagating in orthogonal directions [11].

Perfect chirality (100% emission in a single direction) is frequently pursued by attempting to place the emitter at a point of perfect circular polarisation (a C point). These points are scarce. In nanofibre based waveguides only elliptical polarisation is practically accessible [12], while nano-beam and photonic crystal structures support circular polarisation at a few accessible locations, but the light field is elliptically polarised over the majority of the mode volume [5, 13, 14].

However, in the typical case of elliptical polarisation perfect chiral behaviour is still possible given the correct dipole [8, 12, 15–18]. This suggests the alternative strategy of engineering the emitter dipole, the topic of this letter. This approach is attractive for quantum light-matter interfaces as higher coupling efficiencies will typically be possible using elliptical polarisation.

Emission - We begin with a 1D waveguide supporting a single forward and single backward propagating mode described by classical, complex electric fields $\mathbf{E}_f(\mathbf{r})$ and $\mathbf{E}_b(\mathbf{r})$. Time-reversal symmetry requires, $\mathbf{E}_f = \mathbf{E}_b^*$. Light is emitted by a matter system (MS), modelled as a two level quantum system with energy levels connected by an optical dipole transition with dipole moment $\mathbf{d}$.
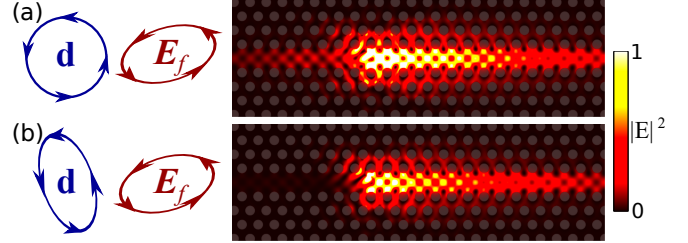
FIG. 1: (a) Simulation of a circular dipole source located at a point of elliptical polarisation in a photonic crystal waveguide. Light is emitted in both directions but the forwards direction is preferred. (b) Replacing the circular dipole source with the depicted elliptical one results in unidirectional emission as this dipole is orthogonal to the polarisation of the backward mode.

The MS could represent an atom or QD for example. It is placed at a location in the waveguide, $\mathbf{r}$, and interacts with the electric fields at this location.

From Fermi's golden rule [19], the likelihood of the excited state decaying via spontaneous emission in the forwards direction is proportional to $|\mathbf{d}^* \cdot \mathbf{E}_f|^2$ while for the backwards direction it is $|\mathbf{d}^* \cdot \mathbf{E}_b|^2$.

When the local polarisation is elliptical, as depicted in Fig.1(a), these dot-product rules indicate that a circular dipole radiates in both directions in the waveguide, but with differing intensities. This is confirmed using a Finite Difference Time Domain simulation, Fig.1(a)[20][21].

However, there will always be a dipole orthogonal to the polarisation of the backwards mode, $\mathbf{d}_\perp^* \cdot \mathbf{E}_b = 0$, so that there is no emission backward. For any polarisation except linear, this dipole will be non-orthogonal to the polarisation of the forwards mode, $\mathbf{d}_\perp^* \cdot \mathbf{E}_f \neq 0$ resulting in emission in only the forward direction [8, 12, 15–18]. An example is shown in Fig.1(b). By setting the dipole's long axis orthogonal to the long axis of the polarisation the linear components have been cancelled, leaving only a circular-like effect (unidirectional emission). This demonstrates that the directional contrast is not in general limited by the degree of circular polarisation, and can be unity with any polarisation (except exactly linear)

given the correct emission dipole.

The chirality can be measured using the directional contrast, the difference between the power radiated forwards and backwards divided by the sum of the two, $D = (|\mathbf{d}^* \cdot \mathbf{E}_f|^2 - |\mathbf{d}^* \cdot \mathbf{E}_b|^2)/(|\mathbf{d}^* \cdot \mathbf{E}_f|^2 + |\mathbf{d}^* \cdot \mathbf{E}_b|^2)$. For a circular dipole it is equal to the (normalised) Stokes parameter describing the degree of circular polarisation $D = S_3 = 2\,\mathrm{Im}(E_x^* E_y)/|\mathbf{E}|^2$ [22]. In figure 2(a) we assess a typical photonic crystal waveguide mode with wavevector $k_x = 0.395(2\pi/a)$, for lattice constant a [23]. The hole radii/slab height are $r = 0.3a$ and $h = 0.6a$ respectively [24]. The polarisation varies spatially, such that a circular dipole is strongly directional ($|D| \geq 0.9$) over small areas as indicated by the darkest shading. However, for each location (except on lines of zero area) there is a dipole that is unidirectional. A specific elliptical dipole is shown, which is "half circular" in the sense that $S_3 = S_1 = 1/\sqrt{2}$, with $S_1 = (|E_y|^2 - |E_x|^2)/|\mathbf{E}|^2$ the Stokes parameter for rectilinear polarisation. It is noticeable that with this dipole a far larger area in the waveguide is useful for unidirectional coupling. Finally we mark the areas for which there exists a dipole that is at least half-circular ($S_3 \geq 1/\sqrt{2}$) which has $|D| \geq 0.9$. This area is ~ 30 times larger than that in which $|D| > 0.9$ occurs with a circular dipole. Had we considered $|D| > 0.95$ the increase would instead be $\sim \times 45$ [19].

The two crucial parameters for a chiral light-matter interface are the directional contrast and the fraction of light that is emitted into the waveguide, known as the Beta factor [25]. We have shown that one can recover high directional contrast with elliptical polarisation. However, it is important to assess how this will effect the Beta factor, which is largely determined by the coupling rate between the MS and waveguide ($\propto |\mathbf{d}^* \cdot \mathbf{E}_f|^2 + |\mathbf{d}^* \cdot \mathbf{E}_b|^2$). Typically a higher electric field intensity will be possible away from a C point [25, 26]. However, away from the C point the polarisations of the forwards and backwards modes are non-orthogonal, and thus the dipole orthogonal to the backward mode has poorer overlap with the forward mode. Accounting for both effects the overall unidirectional coupling strength varies as $S_3^2(\mathbf{r})|\mathbf{E}(\mathbf{r})|^2|\mathbf{d}|^2$.

In Fig.2(b) we explore the impact of these competing effects. At each location the unidirectional coupling rate after the dipole has been adjusted for the new location is plotted. The rate is normalised to the emission rate in bulk GaAs (refractive index $n = 3.45$) to give a Purcell factor; $P(\mathbf{r}) = S_3^2(\mathbf{r})|\mathbf{E}(\mathbf{r})|^2 (3/8\pi v_g f^2 n)$ with f the mode frequency and v_g the group velocity, expressed in units of c/a and c respectively [27]. In Fig.2 $f = 0.262(c/a)$ and $v_g = 0.03c$.

Coupling matching that at a C point is achieved over a significant area, indeed coupling is not maximised at the C points: It is over 50% higher at other locations where increased field intensity has more than compensated for the reduction in overlap between the dipole and the forwards mode. Comparison with part (a) of the figure further shows that the elliptical dipole not only cou-
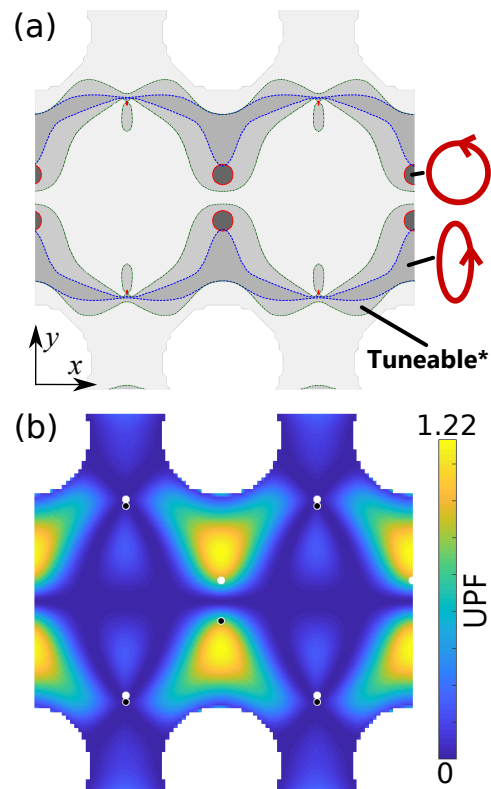
FIG. 2: (a) Positions where different types of dipole source have $|D| \geq 0.9$ in a waveguide mode. Darkest - circular dipole; next darkest - (fixed) elliptical dipole as shown ($S_1 = \sqrt{1/2}$). Second palest - Variable elliptical dipole, tuned for maximum $|D|$ subject to $S_3 \geq 1/\sqrt{2}$ (marked tuneable*). Large white circles - air holes. (b) Unidirectional Purcell factor. White/black dots are right/left polarised C points where unidrectional emission occurs for circular dipoles. In contrast all locations with UPF$\neq 0$ enable unidirectional coupling with suitably elliptical dipoles.

ples unidirectionally in more places, but also does so in places with stronger coupling.

Scattering - Unidirectional coupling also has important consequences for the scattering of photons from the MS. To model scattering we assume that initially the MS is in its ground state and the forwards waveguide mode is populated with a single photon. The scattering amplitudes with which the MS (re)-directs the incident photon are then calculated using a method based on the photonic Green's function. Our aim is to avoid input/output theory which can cause confusion in chiral systems [28]. The calculation is summarised here and detailed in the supplementary information [19].

The interaction between the MS and light is included perturbatively. The probability amplitude in the state $|k\rangle$, $\gamma_k(t)$ at time t is given by $\gamma_k(t) = \sum_{l=0}^{\infty} \gamma_k^{(l)}(t)$, where $\gamma_k^{(0)}$ is defined by the initial condition and all subsequent orders are calculated from the previous according to:

$$\gamma_k^{(z+1)}(T) = \int^T \sum_m \langle k| \hat{H} |m\rangle \frac{\gamma_m^{(z)}(t)}{i\hbar} e^{i(E_k - E_m)t/\hbar} dt, \quad (1)$$

with the sum over all states, E_m the unperturbed energy of the state $|m\rangle$, and H the interaction Hamiltonian [29].

Adopting the long photon limit (a single frequency photon), we can expand the integration range to $\pm\infty$. Further the Hamiltonian is assumed to turn off slowly as $|t| \to \infty$ [30]. This assumption results in each even perturbation order being given by the previous even order times a fixed multiplier, allowing all orders to be collected using a geometric series.

The Hamiltonian for a single optical transition is: $\hat{H} = -i\hat{\sigma}^+\hat{l} + \text{h.c.}$ with [31, 32],

$$\hat{l} = \mathbf{d} \iint \mathbf{G}(\mathbf{r}, \mathbf{r}', \omega') \sqrt{\frac{\hbar \text{Im}[\epsilon(\mathbf{r}', \omega')]}{\epsilon_0 \pi}} \hat{\mathbf{f}}(\mathbf{r}', \omega') d^3\mathbf{r}' d\omega', \quad (2)$$

where $\mathbf{G}(\mathbf{r}, \mathbf{r}', \omega')$ is the tensor electromagnetic Green's function connecting locations $\mathbf{r}$ and $\mathbf{r}'$ at frequency ω'. The raising operator of the MS is $\hat{\sigma}^+$. The dielectric profile is given by ϵ and $\hat{\mathbf{f}}(\mathbf{r}', \omega')$ is the annihilation operator of a bosonic excitation in the dielectric material and its associated electromagnetic field [33].

$\hat{H}$ is inserted into the perturbation model and standard Green's function identities [32, 34, 35], are exploited to simplify the integrals. Finally an integration over a small frequency window is introduced, representing the resolution of a detector. This is necessary to correctly normalise the density of states.

The result is the following equations for the (complex) transmission and reflection amplitudes (the probability amplitudes with which the photon will be found in the forwards/backwards modes in the long-time limit):

$$t = 1 - \frac{\mathbf{d} \cdot \mathbf{E}_f^*(\mathbf{r}) \, \mathbf{d}^* \cdot \mathbf{E}_f(\mathbf{r})}{D}, \quad (3)$$

$$r = -\frac{\mathbf{d} \cdot \mathbf{E}_b^*(\mathbf{r}) \, \mathbf{d}^* \cdot \mathbf{E}_f(\mathbf{r})}{D}, \quad (4)$$

$$D = \frac{1}{2}\left[|\mathbf{d}^* \cdot \mathbf{E}_f(\mathbf{r})|^2 + |\mathbf{d}^* \cdot \mathbf{E}_b(\mathbf{r})|^2\right] + \zeta\left(\mathbf{d} \cdot \mathbf{G}_{\text{Loss}} \cdot \mathbf{d}^* + i\hbar\epsilon_0\Delta\right), \quad (5)$$

where $\mathbf{G}_{\text{Loss}}$ represents the Green's function of the loss mode(s) (with both spatial dependencies set to $\mathbf{r}$) and Δ the detuning between the photon and the transition frequency. The $\mathbf{E}$ terms are the electric fields of Bloch modes normalised as $\int \epsilon(\mathbf{r})|\mathbf{E}(\mathbf{r})|^2 = 1$ with the integration over a single unit cell of the waveguide (or over the cross section for a translationally invariant waveguide like a fibre). In a translationally periodic (invariant) waveguide $\zeta = \frac{2v_g}{a\omega}$ ($\zeta = \frac{2v_g}{\omega}$) with ω the transition angular frequency.

The derivation can be extended to systems with more than two levels and multiple transitions. Consider a four level system with two allowed transitions, one connecting $|g_1\rangle$ to $|e_1\rangle$, and the other $|g_2\rangle$ to $|e_2\rangle$, an arrangement we denote II by analogy to the well known Λ and V systems [36](Fig.4). Here there are two dipoles, $\mathbf{d}_1$, $\mathbf{d}_2$, one for each transition. Similarly there are two detunings. If the system is initially in one of the ground states then equations (3, 4) apply, using the detuning and dipole associated with the transition available to the initial ground state. An initial superposition of ground states simply implies a superposition of reflection/transmission coefficients:

$$(\alpha |g_1\rangle + \beta |g_2\rangle) |1_f\rangle \to$$
$$\alpha |g_1\rangle (t_1 |1_f\rangle + r_1 |1_b\rangle) + \beta |g_2\rangle (t_2 |1_f\rangle + r_2 |1_b\rangle), \quad (6)$$

where r_n, t_n are the reflection/transmission coefficients calculated from equations (3, 4) using the dipole and detuning of the nth transition. This is the underlying mechanism behind some proposals to entangle the emitter with a photon [6].

Scattering calculations for systems where a single ground/excited state has multiple allowed transitions, such as V and Λ arrangements require a more complicated treatment [37, 38]. However, the dot-products that determine directionality are unchanged.

Chiral interactions are characterised not just by an excited MS radiating light in only one direction, but also by a single-photon transmission coefficient that approaches -1 for low loss - i.e. transmission of the incident photon with a phase shift of π. This phase shift is exploited in several proposals for quantum information circuits [6, 14, 39, 40]. It occurs whenever the interaction between the MS and waveguide is unidirectional.

This is shown in Fig.3 where the reflection and transmission coefficients from equations (3, 4) are plotted. In parts (a) and (b) the local polarisation is given by $\mathbf{E}_f = 1/\sqrt{2}\begin{pmatrix}1 & i\end{pmatrix}$ and $\mathbf{E}_f = 1/\sqrt{10}\begin{pmatrix}1 & 3i\end{pmatrix}$ (an arbitrary choice) respectively while along the x axis the dipole is varied as $\mathbf{d} = \begin{pmatrix}\cos\theta & i\sin\theta\end{pmatrix}$ with θ running from 0 to π. A phase-shift ($t \approx -1$) occurs when $\mathbf{d}^* \cdot \mathbf{E}_b = 0$, a consequence of the fact that in this configuration the forwards/backwards emission rates are identical to those with a circular dipole at a C point, indeed there is no special feature that separates chirality with circles from that with ellipses.

More generally, many interesting effects have been predicted in theoretical frameworks where particular forward/backward emission rates are assumed [14, 36, 39–43]. The predictions of these works apply equally well to all polarisation/dipole combinations that produce directionality.

Comparing the points with transmission approaching -1 of parts (a) and (b) of Fig.3 notice the losses are
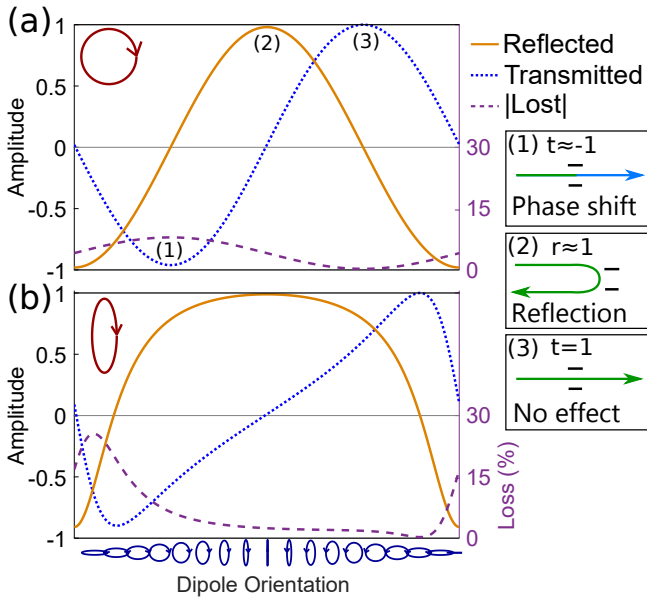
FIG. 3: Single photon reflection (solid) and transmission (dotted) coefficients for a two level MS as a function of the dipole moment. Curves are calculated using equations (3, 4) with $\Delta = 0$, $|\mathbf{E}| = |\mathbf{d}| = 1$ and $\zeta \mathbf{d} \cdot \mathbf{G}_{\text{Loss}} \cdot \mathbf{d}^* = 0.01$. Dashed: lost intensity, right axis. In (a) the polarisation is circular so that a dipole matching the helicity of the light phase shifts a passing photon (1), while a dipole of opposite helicity transmits the photon with no phase shift (3). Linear dipoles reflect the photon (2). In (b) with elliptical polarisation note that there are still dipoles that transmit a photon with or without a phase shift.

higher in (b). Here the poorer dot product between the dipole and the forwards mode, combined with our assumption that $|\mathbf{E}|$ is unchanged between parts (a, b) has led to a reduced Beta factor. However, as discussed previously $|\mathbf{E}|$ can be much higher at elliptical points and this will often more than compensate for the lower overlap. As seen in Fig.2 the choices that maximise coupling (and consequently minimise this loss) are ellipses.

Some proposals require a MS with more than two levels. We consider two specific schemes, both with potential applications in quantum information. First that of [6], which makes use of a charged QD, described as a four-level Π system. Second [36], with Caesium atoms described with three levels in a Λ configuration. In both cases there are two relevant optical transitions and in both ideally one transition couples only to the forwards direction, while the other couples only backwards, depicted in Fig.4. As seen in part (b) of the figure the ideal pair consists of two elliptical dipoles, identical in all respects except for helicity (the arrowhead direction) which is opposite between them. That is, ideally $\mathbf{d}_1 = \mathbf{d}_2^*$ and $\mathbf{d}_1^* \cdot \mathbf{E}_b = 0$.

Note that the non-orthogonality of the dipoles is no impediment to the quantum information proposals, as the orthogonality of dipoles in real space does not equate to orthogonality of quantum states in Hilbert space [19].
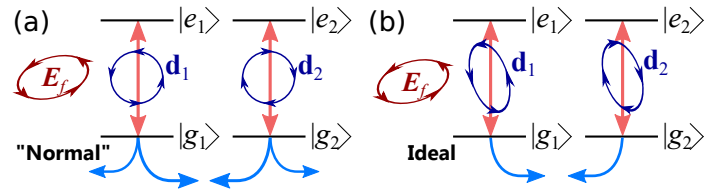
Dipole engineering - Finally we propose illustrative schemes to achieve the necessary dipole engineering in either an atomic or a QD system, focusing on proposals that call for two transitions which are unidirectional in opposite directions [6, 36].

Atoms - Given a system with a circular transition dipole one can imagine rotating the system in 3D space so that the projection of the circular dipole onto the 2D plane spanned by the waveguide mode's electric field resembles the desired ellipse. If provided a system with oppositely circular transitions rotating it to make one transition couple only forwards will result in the other only coupling backward. With atoms in vacuum [36, 44], the external magnetic field defines the quantisation axis, so that the relevant transitions have circular dipole moments in the plane orthogonal to the magnetic field direction [29, 45]. Consequently tilting the applied magnetic field will have the desired effect.

QDs - In QDs there will be in-plane strain, which leads to mixing between the heavy and light holes. The dipole associated with the recombination of an electron with a light-hole has the opposite sense of circular polarisation to that for recombination with a heavy hole. As a result recombination with the mixed holes in the QD is related to an elliptical dipole [46], typically with 1%-20% degree of linear polarization ($\sqrt{1 - S_3^2} = 0.01$–0.2). The dipoles of the two QD transitions are stretched along the same axis, providing the ideal configuration. The degree of linear polarisation in these dipoles can be enhanced to up to 40% by annealing [47], and can be tuned $\pm 20\%$ with application of strain [48]. Two strategies emerge: first, annealing allows the creation of QD-waveguide samples where the (randomly located) QDs are more likely to have a high directionality and stronger waveguide coupling; second, it may be possible to exploit strain-tuning techniques to modify the dipole of a particular QD *in situ* to maximise the directionality.

Conclusion - We propose engineering elliptical dipoles in quantum emitters as an approach to building chiral interfaces. These strategies offer the two-fold advantage

FIG. 4: (a) Four level system with two transitions with opposite circular dipoles. Each interacts with both waveguide directions (arrows). (b) The dipole arrangement such that each interacts with only a single direction. For this polarisation (b) represents the ideal situation for the protocols discussed in the text, in contrast to (a).

of making far more of the space within a waveguide useful for directional interactions while simultaneously enabling a higher photon collection efficiency.

Advanced proposals call for a system with two transitions, each unidirectional but in opposite directions. This requires that the opposite circular dipoles are replaced with ellipses stretched along a shared axis. We have outlined methods to achieve these arrangements in both atomic and QD systems.

In summary, circular polarisations and transition dipoles are not necessary for chiral interactions, furthermore they are typically not the most efficient choices.

Additional references [49–51] are used in the Supplemental information.

* Current address: School of Physics and Astronomy, University of Nottingham, UK

[1] Q. Turchette, R. Thompson, and H. Kimble, Applied Physics B, Supplement **60**, S1 (1995).

[2] A. Auffèves-Garnier, C. Simon, J.-M. Gérard, and J.-P. Poizat, Phys. Rev. A **75**, 053823 (2007).

[3] E. Waks and J. Vuckovic, Phys. Rev. Lett. **96**, 153601 (2006).

[4] A. Aiello, P. Banzer, M. Neugebauer, and G. Leuchs, Nature Photonics **9**, 789 (2015).

[5] R. J. Coles, D. M. Price, J. E. Dixon, B. Royall, E. Clarke, P. Kok, M. S. Skolnick, A. M. Fox, and M. N. Makhonin, Nature Communications **7** (2016), 10.1038/ncomms11183.

[6] A. B. Young, A. C. T. Thijssen, D. M. Beggs, P. Androvitsaneas, L. Kuipers, J. G. Rarity, S. Hughes, and R. Oulton, Phys. Rev. Lett. **115**, 153901 (2015).

[7] K. Y. Bliokh, D. Smirnova, and F. Nori, Science **348**, 1448 (2015).

[8] F. J. Rodríguez-Fortuño, G. Marino, P. Ginzburg, D. OConnor, A. Martínez, G. A. Wurtz, and A. V. Zayats, Science **340**, 328 (2013).

[9] R. Jones, G. Buonaiuto, B. Lang, I. Lesanovsky, and B. Olmos, Phys. Rev. Lett. **124**, 093601 (2020).

[10] P. Lodahl, S. Mahmoodian, S. Stobbe, A. Rauschenbeutel, P. Schneeweiss, J. Volz, H. Pichler, and P. Zoller, Nature **541**, 473 (2017).

[11] I. J. Luxmoore, N. A. Wasley, A. J. Ramsay, A. C. T. Thijssen, R. Oulton, M. Hugues, S. Kasture, V. G. Achanta, A. M. Fox, and M. S. Skolnick, Phys. Rev. Lett. **110**, 037402 (2013).

[12] J. Petersen, J. Volz, and A. Rauschenbeutel, Science **346**, 67 (2014).

[13] M. Burresi, R. J. P. Engelen, A. Opheij, D. van Oosten, D. Mori, T. Baba, and L. Kuipers, Phys. Rev. Lett. **102**, 033902 (2009).

[14] I. Söllner, S. Mahmoodian, S. L. Hansen, L. Midolo, A. Javadi, G. Kiršanskė, T. Pregnolato, H. El-Ella, E. H. Lee, J. D. Song, S. Stobbe, and P. Lodahl, Nature Nanotechnology **10**, 775 (2015).

[15] S. Perea-Puente and F. J. Rodríguez-Fortuño, Phys. Rev. B **104**, 085417 (2021).

[16] M. F. Picardi, A. V. Zayats, and F. J. Rodríguez-Fortuño, Phys. Rev. Lett. **120**, 117402 (2018).

[17] T. V. Mechelen and Z. Jacob, Optica **3**, 118 (2016).

[18] F. J. R.-F. no, D. Puerto, A. Griol, L. Bellieres, J. Martí,

and A. Martínez, Opt. Lett. **39**, 1394 (2014).

[19] T. T. will be the supplementary information, .

[20] A. F. Oskooi., D. Roundy, M. Ibanescu, P. B. Mihai, J. D. Joannopoulos, and S. G. Johnson, Computer Physics Communications **181**, 687 (2010).

[21] Simulation parameters. Structure as fig.2. Source frequency $f = 0.2791(c/a)$. Source position $(x, y) = (-0.125, 0.3958)a$ relative to origin centred on waveguide between two holes. In (a): $\mathbf{d} = 1/\sqrt{2}(1, \mathrm{i})$, (b): $\mathbf{d} = (-0.250 - 0.448\mathrm{i}, 0.856 - 0.061\mathrm{i})$.

[22] B. Lang, D. M. Beggs, A. B. Young, J. G. Rarity, and R. Oulton, Phys. Rev. A **92**, 063819 (2015).

[23] S. G. Johnson and J. D. Joannopoulos, Opt. Express **8**, 173 (2001).

[24] B. Lang, R. Oulton, and D. M. Beggs, J. Opt. **19**, 045001 (2017).

[25] L. Scarpelli, B. Lang, F. Masia, D. M. Beggs, E. A. Muljarov, A. B. Young, R. Oulton, M. Kamp, S. Höfling, C. Schneider, and W. Langbein, Phys. Rev. B **100**, 035311 (2019).

[26] B. Lang, D. M. Beggs, and R. Oulton, Phil. Trans. R. Soc. A **374** (2016), 10.1098/rsta.2015.0263.

[27] V. S. C. Manga Rao and S. Hughes, Phys. Rev. B **75**, 205437 (2007).

[28] For example [52] and [14] draw differing conclusions using input/output theory.

[29] G. Grynberg, A. Aspect, and C. Fabre, *Introduction to Quantum Optics: From the Semi-classical Approach to Quantized Light* (Cambridge University Press, 2010).

[30] J.-T. Shen and S. Fan, Phys. Rev. A **76**, 062709 (2007).

[31] S. Scheel, L. Knöll, and D.-G. Welsch, Phys. Rev. A **60**, 4094 (1999).

[32] R.-C. Ge, C. Van Vlack, P. Yao, J. F. Young, and S. Hughes, Phys. Rev. B **87**, 205425 (2013).

[33] L. Knoll, S. Scheel, and D.-G. Welsch, arXiv:quant-ph/0006121 (2000).

[34] T. Gruner and D.-G. Welsch, Phys. Rev. A **53**, 1818 (1996).

[35] C. Van Vlack, P. T. Kristensen, and S. Hughes, Phys. Rev. B **85**, 075303 (2012).

[36] I. Shomroni, S. Rosenblum, Y. Lovsky, O. Bechler, G. Guendelman, and B. Dayan, Science **345**, 903 (2014).

[37] S. Hughes and G. S. Agarwal, Phys. Rev. Lett. **118**, 063601 (2017).

[38] B. Lang, Thesis (2017).

[39] S. Mahmoodian, P. Lodahl, and A. S. Sørensen, Phys.

Rev. Lett. **117**, 240501 (2016).

[40] T. Li, A. Miranowicz, X. Hu, K. Xia, and F. Nori, Phys. Rev. A **97**, 062318 (2018).

[41] T. Ramos, H. Pichler, A. J. Daley, and P. Zoller, Phys. Rev. Lett. **113**, 237203 (2014).

[42] H. Pichler, T. Ramos, A. J. Daley, and P. Zoller, Phys. Rev. A **91**, 042116 (2015).

[43] I. M. Mirza and J. C. Schotland, Phys. Rev. A **94**, 012302 (2016).

[44] R. Mitsch, C. Sayrin, B. Albrecht, P. Schneeweiss, and A. Rauschenbeutel, Nature Communications **5** (2014).

[45] S. Scheel, S. Y. Buhmann, C. Clausen, and P. Schneeweiss, Phys. Rev. A **92**, 043819 (2015).

[46] A. V. Koudinov, I. A. Akimov, Y. G. Kusrayev, and F. Henneberger, Phys. Rev. B **70**, 241305 (R) (2004).

[47] E. Harbord, Y. Ota, Y. Igarashi, M. Shirane, N. Ku-magai, S. Ohkouchi, S. Iwamoto, S. Yorozu, and Y. Arakawa, Japanese Journal of Applied Physics **52**, 125001 (2013).

[48] J. D. Plumhof, R. Trotta, V. Křápek, E. Zallo, P. Atkinson, S. Kumar, A. Rastelli, and O. G. Schmidt, Phys. Rev. B **87**, 075311 (2013).

[49] R. Loudon, *The Quantum Theory of Light* (OUP Oxford, 1973).

[50] Y. Chen, M. Wubs, J. Mørk, and A. F. Koenderink, New J. Phys **13**, 103010 (2011).

[51] P. Yao, V. Manga Rao, and S. Hughes, Laser & Photonics Reviews **4**, 499 (2010).

[52] Y. Shen, M. Bradford, and J.-T. Shen, Phys. Rev. Lett. **107**, 173902 (2011).